Palaeogeography, Palaeoclimatology, Palaeoecology 299 (2011) 385–398

Contents lists available at ScienceDirect

Palaeogeography, Palaeoclimatology, Palaeoecology

journal homepage: www.elsevier.com/locate/palaeo

Late Eocene sea retreat from the Tarim Basin (west China) and concomitant Asian paleoenvironmental change

Roderic E. Bosboom [a,*], Guillaume Dupont-Nivet [a,b,c], Alexander J.P. Houben [d], Henk Brinkhuis [d], Giuliana Villa [e], Oleg Mandic [f], Marius Stoica [g], Willem Jan Zachariasse [h], ZhaoJie Guo [b], ChuanXin Li [b], Wout Krijgsman [a]

[a] Paleomagnetic Laboratory Fort Hoofddijk, Faculty of Geosciences, Utrecht University, Budapestlaan 17, 3584 CD Utrecht, The Netherlands
[b] Key Laboratory of Orogenic Belts and Crustal Evolution, Ministry of Education, Peking University, Beijing 100871, China
[c] Géosciences Rennes, UMR 6118, Université de Rennes1, Campus de Beaulieu, 35042 Rennes Cedex, France
[d] Biomarine Sciences, Institute for Environmental Biology, Faculty of Science, Utrecht University, Laboratory for Palaeobotany and Palynology, Budapestlaan 4, 3584 CD Utrecht, The Netherlands
[e] Dipartimento di Scienze della Terra, University of Parma, Viale Usberti, 157A, 43100 Parma, Italy
[f] Geological-Palaeontological Department, Natural History Museum Vienna, Burgring 7, A-1010 Wien, Austria
[g] Department of Geology and Paleontology, Faculty of Geology and Geophysics, Bucharest University, B lcescu Bd. 1, 010041, Romania
[h] Stratigraphy-Paleontology, Department of Earth Sciences, Utrecht University, Budapestlaan 4, 3584 CD Utrecht, The Netherlands

ARTICLE INFO

Article history:
Received 5 July 2010
Received in revised form 19 November 2010
Accepted 22 November 2010
Available online 29 November 2010

Keywords:
Tarim Basin
Paratethys
Paleoenvironment
Biostratigraphy
Eocene

ABSTRACT

The Paleogene sediments of the southwest Tarim Basin along the West Kunlun Shan in western China include the remnants of the easternmost extent of a large epicontinental sea. This shallow sea once extended across the Eurasian continent before it retreated westward and eventually separated as the Paratethys Sea. Climate modeling results suggest that this sea retreat is an equally important forcing mechanism as the Tibetan plateau uplift in the aridification of the Asian continental interior and the intensification of the Asian monsoon system. The age and paleogeography of the retreat are poorly constrained, hindering the understanding of its cause and paleoenvironmental impacts. This study reports litho- and biostratigraphic results from two sections recording the last major regression out of the Tarim Basin that is expressed by a regional transition from marine clastics and limestones to continental red-beds. Rich micro- and macrofossil assemblages, including benthic foraminifera, ostracods, bivalves, calcareous nannofossils and organic walled dinoflagellate cysts (dinocysts), indicate a shallow, proximal and marine environment. Strong similarity to assemblages known from Central Asia and Europe confirms that surface–ocean connections extended across Eurasia from the Tarim Basin to the western Tethys during the latest Eocene. Moreover, the recovered fossil associations date the last marine sediments as earliest Priabonian in age (~37 Ma; overlap between dinoflagellate Mps Interval Zone and calcareous nannofossil Zone CP 14). The retreat of the sea from the Tarim Basin is time-equivalent with the sea level lowstand at the Bartonian–Priabonian boundary but pre-dates both the Oligocene–Miocene regional uplift of the Pamir mountains and Kunlun Shan and the major eustatic sea-level falls of the Eocene–Oligocene Transition (~34 Ma) and mid-Oligocene (~30 Ma), which are usually held responsible for the sea retreat. Furthermore, a concomitant and significant aridification step occurs at ~36.6 Ma (top of chron C17n.1n) as recorded by regional sedimentary records of the Xining Basin along the northeastern Tibetan Plateau, suggesting that the Tarim Sea served as a significant moisture contributor for the Asian interior.

1. Introduction

Asian paleoenvironment and climate are commonly interpreted to be mainly governed by the formation of the Tibetan Plateau in response to the Indo-Asia collision. This drastic increase in topography is thought to have provoked aridification of the vast Asian interior, since the related changes in atmospheric circulation intensified continentality and strengthened the Asian monsoon system (Boos and Kuang, 2010; Graham et al., 2005; Kent-Corson et al., 2009; Kutzbach et al., 1989; Prell and Kutzback, 1992; Ruddiman and Kutzbach, 1989; Sun and Wang, 2005). On the other hand, general circulation models show that tectonic forcing may be minor compared to the effects of the redistribution of the land–sea thermal contrast associated with the westward retreat of the vast shallow epicontinental sea that formerly covered large parts

* Corresponding author. Tel.: +31 30 253 5246.
E-mail address: R.E.Bosboom@geo.uu.nl (R.E. Bosboom).

0031-0182/$ – see front matter © 2010 Elsevier B.V. All rights reserved.
doi:10.1016/j.palaeo.2010.11.019

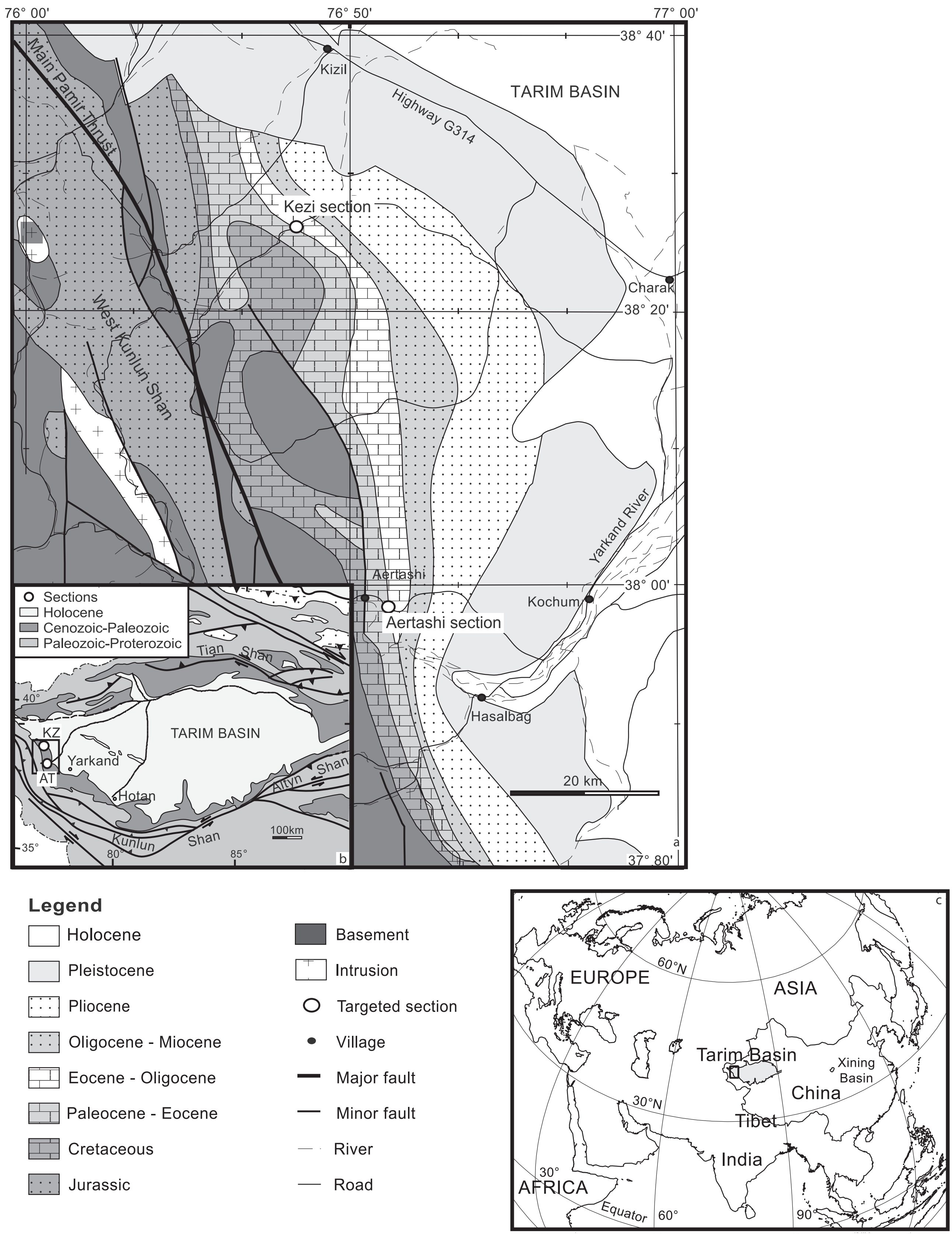

Fig. 1. Simplified geological map of the field area (a) showing lithostratigraphic units, tectonic features and locations of the Aertashi (AT) and Kezi (KZ) sections (modified from the 1:500.000 scale map of the Bureau of Geology and Mineral Resources of Xinjiang Uygur Autonomous Region, 1993). The inset (b) shows the location of the study area within a schematic geologic map of the Tarim Basin displaying major lithostratigraphic units and tectonic features (modified from Dupont-Nivet et al., 2002). The locations of the Tarim and Xining Basins are shown on the large-scale map of Eurasia (c; present-day coastal outline obtained from GPlates 0.9.7.1).

of the Eurasian continent (Garzione et al., 2005; Graham et al., 2005; Kent-Corson et al., 2009; Ramstein et al., 1997; Zhang et al., 2007). This sea is presumed to have belonged to the Tethyan Realm (Dercourt et al., 1993; Mao and Norris, 1988; Popov et al., 2004; Rögl, 1999) and extended as far east as the Tarim Basin during Paleogene times (Fig. 1). The mechanisms underlying the retreat of this Tarim Sea (also referred to as 'Tajik Sea' or as a bay of the 'Turan Sea' by Burtman, 2000; Burtman and Molnar, 1993; Tang et al., 1992) are poorly understood and generally interpreted as a relative sea-level fall enforced by Indo-Asia collision tectonics. The initial tectonic uplift of the Pamir mountains, the West Kunlun Shan (= mountain range) and the Tian Shan could have resulted in sedimentary overfilling and separation of the Tarim Basin from the adjacent basins to the west (Fig. 1; Burtman, 2000; Burtman and Molnar, 1993; Coutand et al., 2002; Hao and Zeng, 1984; Lan, 1997; Tang et al., 1992). Alternatively, the Tarim Sea retreat could have been caused by a major Paleogene eustatic regression like the mid-Oligocene sea-level fall at ~30 Ma (Haq et al., 1987) as first proposed by Sobel and Dumitru (1997) or the Eocene Oligocene Transition (EOT) at ~34 Ma, associated with global cooling and Antarctic ice sheet formation (e.g. Brinkhuis, 1994; Coxall et al., 2005; Escutia et al., 2010; Katz et al., 2008; Lear et al., 2008; Miller et al., 2005; Pagani et al., 2005; Pearson et al., 2009) as put forward by Dupont-Nivet et al. (2007). However, both the age and paleogeography of the Tarim Sea retreat are currently too poorly constrained to properly evaluate its controlling mechanisms (i.e. tectonically-induced sea-level fall vs. eustatic sea-level fall) and paleoenvironmental impacts.

This study therefore focuses on the Paleogene sediments of the southwest Tarim Basin which record the last major retreat of the Tarim Sea (Jin et al., 2003; Sobel, 1999; Yin et al., 2002). The regional Paleogene stratigraphy is presently incomplete and the previous age estimates of the final retreat range from the middle Eocene to the late Oligocene (Lan and Wei, 1995; Mao and Norris, 1988; Yang et al., 1995; Zhong, 1992). Hence, here we aim to construct an improved regional stratigraphic framework of the last major Tarim Sea regression using multiple biostratigraphic constraints from key sedimentary successions. This framework will elucidate both the cause and the paleoenvironmental impacts of the paleogeographic changes associated to the retreat of the Tarim Sea.

2. Geological setting

The sedimentary deposits recording the marine to continental transition are located along the southwestern margin of the Tarim Basin in the foothills of the West Kunlun Shan fold-and-thrust belt, which is along the northwestern rim of the Tibetan Plateau in west China (Fig. 1).

2.1. Tectonic setting

The Tarim Basin is part of a relatively undeformed crustal block within the Indo-Asia collision system (Yin and Harrison, 2000). Its sedimentary infill rests on a basement of supposedly Archean and Proterozoic oceanic crustal fragments mainly composed of crystalline metamorphic gneisses (Tian et al., 1989). The overlying platform carbonates and fine-grained clastics of the Paleozoic and the mainly coarse-grained clastics of the Mesozoic have been strongly deformed by the successive accretion of continental terranes, which started during late Triassic and ended by the Eocene Indo-Asia collision (Hendrix et al., 1992; Jia et al., 2004; Robinson et al., 2003; Yin and Harrison, 2000). The Cenozoic northward movement of India into Eurasia continues until today and has resulted in the marginal overthrusting of the Tarim Basin by the Tian Shan in the north, the Pamir mountains in the west and the Kunlun Shan in the south (Fig. 1; Burtman and Molnar, 1993; Cowgill, 2010; Jia et al., 1997; Yin and Harrison, 2000). It is thought that initial tectonic flexural loading in the late Cretaceous resulted in the formation of two major distal foreland basins, one along the southern margin of the Tian Shan and one along the northeastern margin of the West Kunlun Shan with its depositional centre near Yarkand, the focus of this study (Fig. 1; Jia et al., 1997; Yang and Liu, 2002). Thrusting and exhumation of the Pamir and West Kunlun Shan initiated sometime between the late Eocene and early Miocene according to sedimentologic (Burtman, 2000; Yin et al., 2002), thermochronologic (Sobel and Dumitru, 1997), paleomagnetic (Thomas et al., 1994; Yin et al., 2002), and back-stripping (Yang and Liu, 2002) data. However, the general consensus is that the rapid uplift and topographic expression of the Pamir–Kunlun system did not occur until late Oligocene–early Miocene as

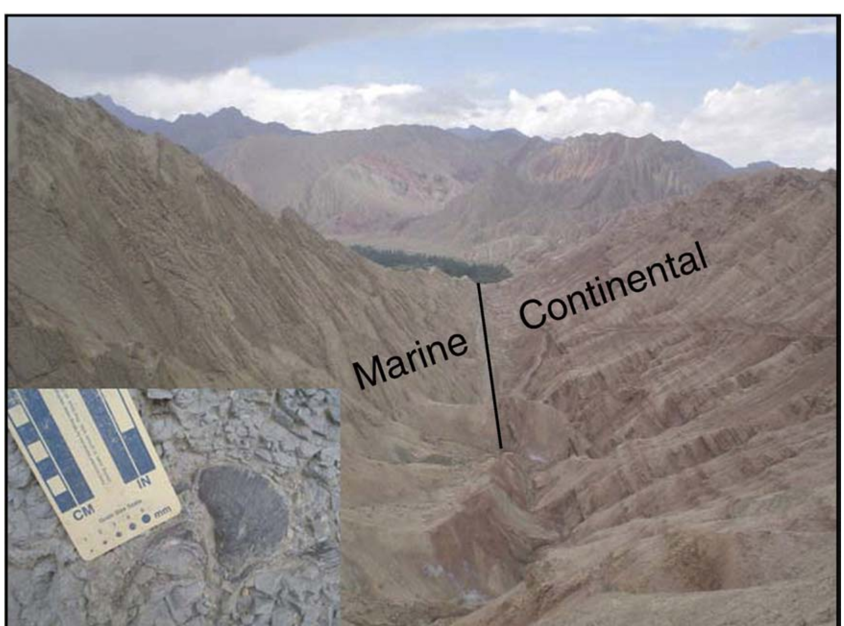

Fig. 2. Field view of the Aertashi section (road for scale) showing the transition from the green-colored deposits of marine origin to the continental red-beds. The inset shows typical oysters (*Sokolowia buhsii*) from the marine Wulagen Formation (table for scale).

the evidence for an early uplift is sparse and not well constrained (see Cowgill (2010) for a review). The southwest Tarim Basin subsequently developed into a proximal foreland depression experiencing high accumulation rates due to this acceleration of basinward thrusting and overloading of the Kunlun Shan. This late phase of overthrusting has weakly deformed the Cenozoic strata, mainly coarse-grained clastics, which discordantly overlie the Mesozoic sediments. The present-day Tarim Basin has evolved into the largest intracontinental basin of China and the largest closed drainage basin in the world.

2.2. Stratigraphic setting

It is generally reported that the sea invaded the Tarim Basin during the Cenomanian from the neighboring basins in the west through the present-day Alai Valley (Burtman, 2000; Burtman and Molnar, 1993; Tang et al., 1992), though marine fossils have been described from lower Cretaceous sediments (Guo, 1991). A total of five late Cretaceous to Paleogene major marine incursions have been distinguished from the sedimentary record in the westernmost part of the Tarim Basin, west of Kashgar (Fig. 1; Burtman, 2000; Burtman et al., 1996; Lan and Wei, 1995; Tang et al., 1989). Previous studies of the marine record show that the eastward extent of these incursions into the Tarim Basin varied through time, increasing from the first incursion till a maximum was reached by the supposedly early Eocene third transgression and then decreasing again until the final fifth incursion (Fig. 3; Burtman, 2000; Burtman et al., 1996; Lan and Wei, 1995; Tang et al., 1989). Our study focuses on the fourth transgression as this is the last major incursion extending well into the Tarim Basin, whereas the fifth transgression has only been recognized along the westernmost margin of the basin, west of Kashgar (Fig. 1; Lan, 1997; Lan and Wei, 1995).

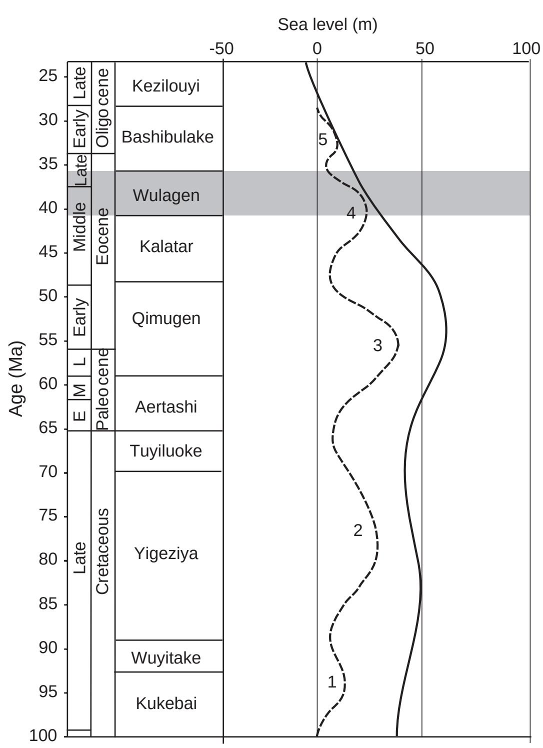

Fig. 3. Schematic regional framework of the five marine incursions in the Tarim Basin based on a review of existing Chinese literature (see text). The approximate relative changes in sea-level are reflected by the dotted line, whereas the long-term sea-level curve relative to present-day sea-level is shown by the bold line corresponding to the top scale (Miller et al., 2005; Watts and Steckler, 1979). Note that the age and relative sea-level of each cycle (which is simply based upon the reported eastward extent of each incursion into the basin) are inexact, but generally do fit the long-term eustatic trend. The shaded area highlights the Wulagen Formation corresponding to the last major sea retreat from the basin paleo-depocentre, the focus of this study.

The transgressive intervals are dominated by subtidal facies, particularly shallow marine, carbonate platform and tidal flat deposits comprising grey and green limestones, dolomites, mudstones and sandstones (Mao and Norris, 1988; Tang et al., 1989). These deposits are characterized by distinct fossil assemblages of mostly bivalves, dinoflagellate cysts and ostracods, enabling inter- and intra-basin stratigraphic correlations (e.g. Lan and Wei, 1995; Mao and Norris, 1988; Tang et al., 1989; Yang et al., 1995). The regressive intervals in between consist mostly of supratidal and intertidal lagoonal and (evaporative) tidal flat facies dominated by massive gypsum beds and brownish-red gypsiferous mudstones (Mao and Norris, 1988; Tang et al., 1992).

The designation of regional stratigraphic units of marine origin is not uniform. In this study, the nomenclature of Lan and Wei (1995) and Yin et al. (2002) is used. Accordingly, the marine sequence of Paleogene age is referred to as the Kashi Group, which comprises in chronological order the Aertashi, Qimugen, Kalatar, Wulagen and Bashibulake Formations (Table 1). The overlying stratigraphic unit is the continental Kezilouyi Formation of the Wuqia Group. The Kashi Group records the last three transgression–regression cycles: the third cycle from the Aertashi to the Qimugen Formation, the fourth cycle from the Kalatar to the First Member of the Bashibulake Formation and the minor fifth cycle from the Second to the Fifth Member of Bashibulake Formation, which has only been reported from the westernmost Tarim Basin (Lan, 1997; Lan and Wei, 1995; Sobel and Dumitru, 1997; Yin et al., 2002). See Table 1 for a comprehensive and detailed overview of the lithostratigraphy, corresponding thicknesses, age estimates and transgression–regression cyclicity.

In this study we review and update the marine biostratigraphy focusing on the last major regression associated to the fourth incursion that has been assigned conflicting ages by previous biostratigraphic studies (Fig. 3). The last marine deposits of this incursion belong to the Wulagen Formation (Table 1), for which age estimates range from late middle Eocene based upon calcareous nannofossils (Zhong, 1992), bivalves (Lan and Wei, 1995) and ostracods (Yang et al., 1995) to late Eocene based upon dinoflagellate cysts (Mao and Norris, 1988). This marine to continental transition is particularly well exposed in the area near Yarkand (Fig. 1), close to the paleo-depocentre of the West Kunlun Shan foreland basin (Hu, 1992; Jia et al., 1997; Yang and Liu, 2002) with an overall thickness of the marine deposits in excess of ~1500 m. The shift to continental conditions is easily recognized (Fig. 2), grading upwards from the green-colored marine deposits to mainly red-beds comprising mudstones, siltstones, sandstones and gypsum interbeds of fluvial and lacustrine origin (Jia et al., 2004; Zheng et al., 2006).

3. Lithostratigraphy of sampled sections

In the summer of 2007 two sections, separated laterally by ~50 km, have been studied to establish the stratigraphic framework of the Tarim Sea retreat. The sections, referred to as the Aertashi and Kezi sections (named after the nearby villages) were chosen based on their continuity and location close to the paleo-depocentre of the basin, providing the highest stratigraphic recovery (Fig. 1). The Aertashi section (37°58'N, 76°33'E) is well-exposed along the Yarkand River and along the road from Kochum to Aertashi (Fig. 2). The Kezi section (38°26'N, 76°24'E) is exposed along the Kezi River and its tributary streams. The strata at both localities are exposed continuously with consistent homoclinal ~25–35° westward dip.

The Aertashi section has been the focus of earlier studies. Yin et al. (2002) proposed a stratigraphic framework of the Neogene based upon magnetostratigraphy and detrital fission track dating. Sobel and Dumitru (1997) primarily focused on detrital fission track dating of the Jurassic to Neogene successions. Kent-Corson et al. (2009) report

Table 1
Simplified lithostratigraphic description and transgression–regression cyclicity for the western Tarim Basin of the Paleogene. The lithostratigraphy and corresponding thicknesses (not to scale) are summarized from Jia et al. (2004), Mao and Norris (1988) and Tang et al. (1989), whereas the preliminary age estimates are based upon calcareous nannofossils (Zhong, 1992), bivalves (Lan and Wei, 1995), ostracods (Yang et al., 1995), dinoflagellate cysts (Mao and Norris, 1988) and benthic foraminifera (Hao and Zeng, 1984). The shaded area shows the Wulagen Formation on which this study primarily focuses.

System	Formation			Thickness	Age	Lithology	Cyclicity
PALEOGENE	Wuqia Group	Kezilouyi Fm		200-500 m	Oligocene-Miocene	red-beds including mudstones, siltstones, sandstones and gypsum interbeds	Continental
	Kashi Group	Bashibulake Fm	5	65 m (east) -380 m (west)	late Eocene-late Oligocene	brownish red-mudstones intercalated by siltstones, thin beds of gypsum and fine-grained sandstones with occasional ripple marks and cross-bedding.	5th regression (final)
			4			brownish-red mudstones with interbeds of siltstones, thinly bedded gypsum and grayish-green sandy shell beds	5th transgression (final)
			3		late Eocene-early Oligocene		
			2				
			1				4th regression
		Wulagen Fm		10-180 m	late middle Eocene	grayish-green mudstones intercalated with thin shell beds, shelly limestones and muddy siltstones, occasionally overlain by massive white gypsum beds interbedded with brownish-red mudstones and siltstones	4th transgression
		Kalatar Fm		25 m (east) -180 m (west)	middle Eocene	grey massive limestones, marls and grayish-green mudstones with interbeds of shelly limestones, oolitic limestones, shell beds and gypsum	
		Qimugen Fm	Upper	20 (east) -130 m (west)	late Paleocene-early Eocene	brown gypsiferous mudstones and muddy massive gypsum beds intercalated with yellowish-green mudstone	3rd regression
			Lower		middle-late Paleocene	grayish-green mudstone intercalated with thin-bedded shelly limestone	3rd transgression
		Aertashi Fm		20-440 m	early Paleocene	massive gypsum beds intercalated with gypsiferous miudstones and dolomitic limestones	

stable isotope analyses on the Cenozoic stratigraphy. The Kezi section is close or identical to the Qimugen section which has been studied previously by Jin et al. (2003) and Mao and Norris (1988).

Both studied sections intersect the same stratigraphic units of Paleogene age within the overall transition from grayish-green marine to reddish-brown continental beds (Fig. 1). This initial stratigraphic correlation is supported by the recognition of five distinctive lithostratigraphic units with very similar facies and thicknesses at both sections. The Aertashi section comprises Units 2 to 5, whereas Units 1 to 5 have been sampled at Kezi (Fig. 4). Note that this correlation is solely a lithostratigraphic correlation and not necessarily an age correlation. These stratigraphic correlations will be further assessed in light of biostratigraphic data presented below.

The stratigraphic thicknesses of the recognized lithostratigraphic units (Fig. 4) were measured to decimetric precision. The zero meter level of both sections is defined by the last green-colored shell bed within the fourth unit. Grey massive limestones with shell interbeds constitute Unit 1 (base to −115 m level at Kezi). Unit 2 (base to −45 m level at Aertashi; −115 to −40 m level at Kezi) comprises massive calcareous green sandstones and grey limestones with shell beds at their top, which are interbedded with green mudstones. Unit 3 (−45 to −25 m level at Aertashi; −40 to −20 meter level at Kezi) is characterized by green mudstones and occasional shell beds. The boundary between Units 3 and 4 is easily recognized in the field by a clear change in color from green to red (Fig. 2). A thick interval of red laminated mudstones interbedded with shell beds and irregular bedded green calcareous (bioturbated) siltstones and fine sandstones rich in fossils characterizes Unit 4 (−25 to 10 m level at Aertashi; −20 to 10 m level at Kezi). Unit 5 (10 m level to top at Aertashi; 10 m level to top at Kezi) consists of red laminated mudstones interbedded with increasingly dominant siltstones and fine sandstones with local ripple marks, slightly incised channel fills and nodular gypsum. This change between Units 4 and 5 from fine-grained beds dominated by marine fossil assemblages to coarser-grained beds characterized by sedimentary flow structures marks the transition from a mostly marine to a more continental depositional environment (Fig. 4).

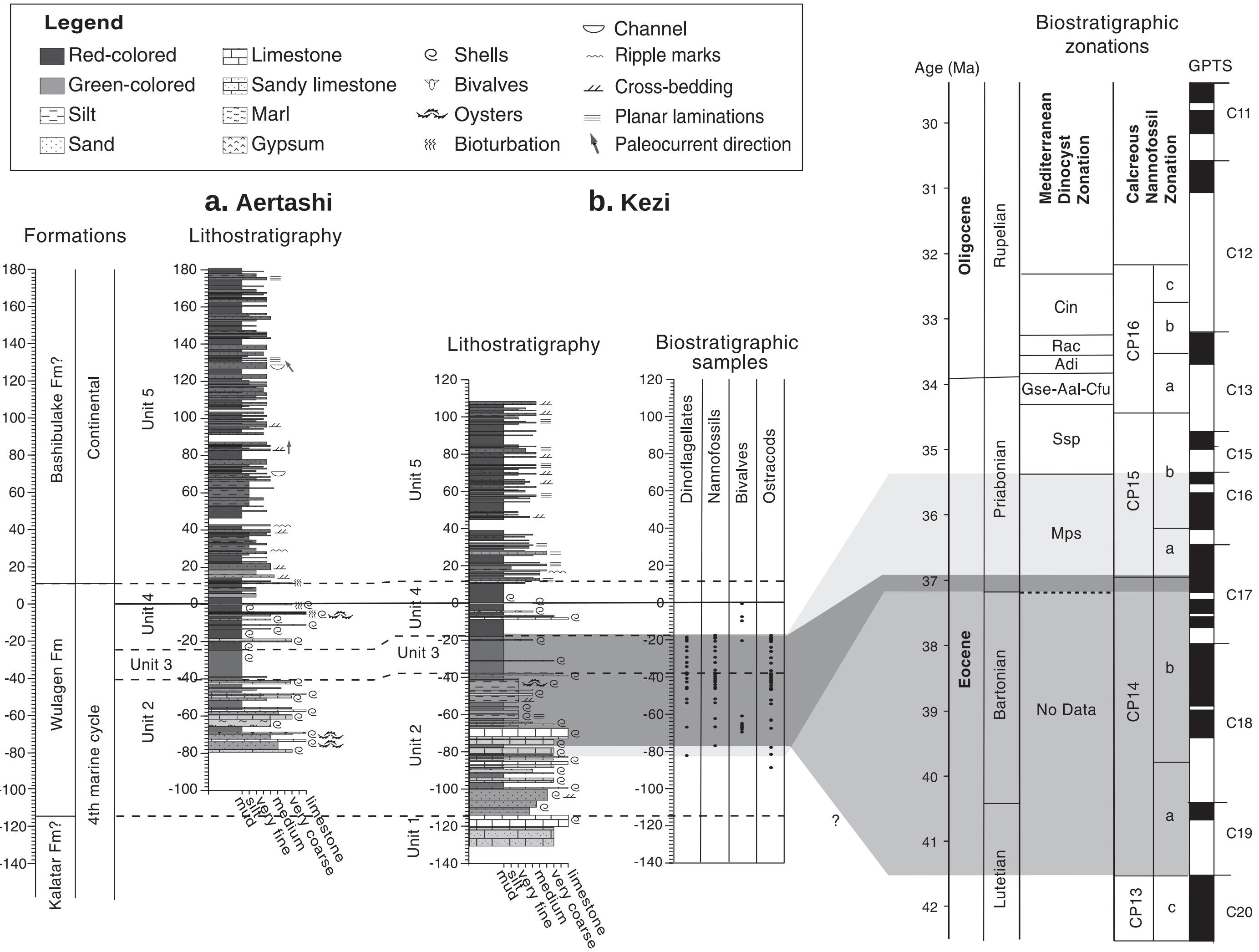

Fig. 4. Lithostratigraphy and biostratigraphic correlations for the Aertashi (a) and Kezi sections (b). The correlation between the two sections are indicated by the dotted lines and the sedimentary units. Zero level is defined by the last green-colored shell bed. On the left is the correlation to the regional stratigraphic framework of the southwest Tarim Basin. On the right is the correlation to the Western Tethys dinoflagellate zonation (after Brinkhuis and Biffi, 1993), global calcareous nannofossil zonation and geomagnetic polarity time scale (Gradstein et al., 2004). The shaded area indicates the widest possible age-range provided by assignment to calcareous nannofossil zone CP 14 (dark shaded zone) and the dinoflagellate Mps Interval Zone (light shaded zone). The overlap between these two shows the most likely age of the Tarim Sea retreat is earliest Priabonian at approximately ~37 Ma.

Comparison of our description of the lithostratigraphy with that of previous studies (Table 1) shows that Units 2 and 3 with a total thickness of ~100 m hold strong resemblance with the Wulagen Formation described from sections along the southwest Tarim Basin. This subtidal sequence with a thickness of up to ~130 m comprises mostly green mudstones intercalated by siltstones and shelly limestones and has been deposited during the fourth transgression–regression cycle (Lan and Wei, 1995; Mao and Norris, 1988; Tang et al., 1989; Zhong, 1992). Unit 1 thus likely represents the massive limestones of the underlying Kalatar Formation, whereas Unit 4 would correspond either to the package of red clastics and gypsum beds occasionally overlying the Wulagen Formation (though gypsum is not present in our sections) or to the red continental members of the Bashibulake Formation (Fig. 4; Lan and Wei, 1995; Mao and Norris, 1988).

Preliminary facies analyses indicate the lithostratigraphy of both sections constitute part of a shallowing-upward cycle (or cyclothem) typical for shallow epicontinental seas, with subtidal carbonate platforms at its base, (lagoonal) intertidal plain deposits constituting the middle part, and alluvial floodplain red-beds at the top (Fig. 4; Aigner et al., 1990; Reading, 2006). The alternation of siliciclastics and carbonate suggests that superimposed on the overall shallowing upward trend, high-frequency fluctuations in relative sea-level or sediment supply result in lowstand siliciclastic shedding and highstand carbonate build-up (Budd and Harris, 1990; Reading, 2006). The overall similarity between the Aertashi and Kezi sections in terms of lithostratigraphy shows that this shallowing upward trend occurred basin-wide.

4. Biostratigraphy

The samples for foraminifer, ostracod, bivalve, calcareous nannofossil and organic walled dinoflagellate cyst (dinocyst) analyses were collected from representative marine beds throughout Units 2 to 4 (Fig. 4). In general, age correlations are based upon the standard macro- and microfossil zonations of the geologic time scale by Gradstein et al. (2004).

4.1. Foraminifers

Foraminifers were studied from the washed residues of 25 samples. Residues are generally small with the exception of a few samples. Most residues are made up almost entirely of benthic foraminifers with minor additions of ostracods and occasionally of sea urchin spines. Any upward trend in the overall composition is absent. The overall benthic foraminiferal fauna is made up of representatives of the genera *Cibicides* (both biconvex and planoconvex types), *Anomalinoides*, *Textularia*, *Nonion* and/or *Protelphidium*, *Cancris*, and miliolids with rare admixtures of representatives of *Brizalina*, *Hanzawaia*, *Asterigerina* and *Lenticulina*. This association is indicative of a vegetated inner neritic environment (<100 m water depth) in agreement with the absence of planktonic foraminifers (Fig. DR1; Murray, 1991).

4.2. Ostracods

The studied ostracod fauna is based on 30 micropaleontological samples collected from Units 2 to 4 of the Kezi section (Fig. 4). In general, ostracods from these samples are rare and badly preserved as most of the ornamentation has been dissolved. This made a precise discrimination of the taxa somewhat difficult. Nonetheless, few samples that provided a relatively rich and well-preserved ostracod fauna, enabled some biostratigraphical and taxonomic observations (Fig. DR2).

4.2.1. Biostratigraphic considerations

The majority of the samples from Unit 2 are almost barren of ostracods, which makes it difficult to attribute the ostracod assemblage to published ostracod zonations. The main species recorded at this level are represented by *Cytherella compressa* (von Münster), *Cytherella draco* Pietrzeniuk, *Paracypris bouldnorensis* Keen, *Haplocytherideа curvata* (Lienenklaus), *Schuleridea perforata perforata* (Roemer), *Schuleridea* sp., *Rugieria semireticulata* Haskins, *Cytheretta vulgaris* var. "tricostulée" Ducasse, *Eocytheropteron* sp., *Loxoconcha delemontensis* Oertli, *L.* sp., *Eucytherura hyonensis* Keij, *Krithe* cf. *bartonensis* (Jones), *Buntonia* sp., *Hazelina* cf. *indigena* Moos and *Paijenborchella* cf. *tricostata* (Lienenklaus). Some of these species have been recorded also in Paleogene sediments from European basins (e.g. Bombita and Rusu, 1981; Ducasse et al., 1985; Keen, 1978; Keij, 1957; Olteanu, 2006; Pietrzeniuk, 1969; Scheremeta, 1969; Szczechura, 1977; Yeşilyurt et al., 2009). The stratigraphic distribution of these species differs from one author to another but generally they are regarded as indicators for the late Eocene.

The ostracod fauna from the upper part of Unit 3 and mainly Unit 4 is dominated by species of the genus *Cytheridea*, the most common being *Cytheridea* sp. ex. gr. *Cytheridea pernota* (Oertli & Keij). This species shows similarities with *C. pernota* (Oertli & Keij), which has been recorded from lower Oligocene deposits in western Europe, but also has some common features with *Cytheridea intermedia* (Reuss) described in the same area from late Eocene (Ducasse et al., 1985; Keen, 1978; Keij, 1957; Olteanu, 2006). Additionally, few specimens of *Krithe* cf. *bartonensis* (Jones), *Paracypris* sp., *Eucytherura keiji* Pietrzeniuk, *Haplocytheridea helvetica* (Lienenklaus) and *Cytherura alata* (Lienenklaus) have been recognized, of which the latter two have been reported to be of early Oligocene age (Oertli, 1956; Olteanu, 2006).

Summarizing, in view of the uncertainties in the determination of and the sensitivity of ostracods to environmental control, preliminary age estimates range from late Eocene to earliest Oligocene.

4.2.2. Paleoenvironmental analysis

The ostracod assemblages indicate proximal shallow water conditions and normal marine salinity. Particularly, *Cytheridea* spp. is characteristic for a shallow marine environment (van Morkhoven, 1963), although some taxa (including *Krithe* cf. *bartonensis* (Jones) and *Cytherura alata* (Lienenklaus) are also found in deeper waters (Yeşilyurt et al., 2009). The massive presence of echinoids plates and spines in the micropaleontological samples are also an indication of proximal marine conditions. The ostracod distribution further shows the presence of two short transgressive pulses around −20 m level and −33 m level by the regeneration of microfauna (Fig. 4). These pulses show that higher order variability in sea-level is superimposed on the overall shallowing upward trend recognized from the lithostratigraphy.

4.3. Bivalves

Mollusk macrofaunas have been collected from six horizons of the Kezi Section (Fig 4; −68.5 to −64.7 m level, −60.6 m level, −20.0 m level, −8.5 m level, −7 m level and −0.1 m level) and two horizons of the Aertashi section (Fig. 4; −28.1 m level and −2.0 m level). The samples are dominated by oysters, likely because all aragonite mollusk representatives were secondarily leached. Therefore this study concentrates on the evaluation of oysters (Ostreidae), a group of epifaunal pteriomorph bivalves producing predominantly calcite shells (Stenzel, 1971). Taxonomic identification follows largely the species-concepts established by Lan and Wei (1995) representing the most current revision of abundant regional systematic literature (Fig. DR3).

4.3.1. Biostratigraphic considerations

The lowermost sample in both sections is dominated by *Kokanostrea kokanensis*. Except for the −20.0 m level horizon of the Kezi section, other samples are dominated by different *Flemingostrea* species. The −20.0 m level sample comprises one single articulated, well-preserved specimen of *Sokolowia buhsii* morph. *alpha*. As it is articulated (preserved with valves closed), shows no abrasion of the shell surface and has been recovered from a low-energy marl, it must be *in situ* (Fig. 2). The debris material of both sections included a number of representatives of *Sokolowia*, *Kokanostrea* and *Flemingostrea* individuals. *Flemingostrea* is well represented within the lowermost sample of the Kezi section (abundant *F. kaschgarica*). The horizon above *Sokolowia* comprises *F. schurabica* (also referred to as *F. kaschgarica ulugqatensis*). Further upsection follows badly preserved *F. yengisarica* together with *K. kokanensis*, whereas the topmost sample comprises both *F. yengisarica* and *F. kashgarica*. The uppermost sample of the Aertashi section, taken from a red marl horizon, bears the same two taxa. According to Lan and Wei (1995) and Lan (1997) such faunal composition places the samples into the Wulagen Formation, in particular into its lower and middle part characterized by *Sokolowia*–*Kokanostrea* assemblage.

Further west (see paleogeographic discussion below), in the Ferghana Basin in eastern Uzbekistan the *Sokolowia buhsii* (there as *S. esterhazyi*) horizon within the Ferghana Group defines stratigraphically the Turkestan Stage (Vyalov, 1935). Indeed, Vyalov (1937) proposed the new regional stage name Turkestanian defined by range zones of *S. esterhazyi*, *S. romanowskyi*, *S. boehmi*, *K. kokanensis* and *F. schurabica*, suggesting that this stage can be used in other parts of Central Asia, including the Tarim Basin. *Sokolowia* is described from Irkeshtam (Kyrgyzstan) by Böhm (1903) and from the Syr Darya Basin in Kazakhstan by Romanovski (1880) and Gorizdro (1913). In the southern Afghan–Tajik Depression in northwest Afghanistan *Sokolowia* is common in the Ambar Koh Formation of which the topmost beds have been dated by means of planktonic foraminifera to the Mid-Bartonian P14 Zone (Berizzi Quarto di Palo, 1970; Cita and Premoli Silva, 1975; Desio and Martina, 1975; Gradstein et al., 2004; Premoli Silva, 1970; Rossi Ronchetti, 1975). Beds with *Sokolowia* from the Bathyz Formation in southeast Turkmenistan are correlated to the Lutetian-lowermost Priabonian *Reticulofenestra umbilica* nannofossil Zone (CP 14 to CP 15; Fig. 4; Bugrova, 2009; Gradstein et al., 2004). In the Transylvanian Basin of Romania *S. buhsii* (= *esterhazyi*) (Meszaros, 1957; Pavay, 1871) is found in the lower part of the Capusu Formation (Rusu et al., 2004). The co-occurrence of planktonic foraminifera of the P12 Zone and calcareous nannoplankton of the Zone NP16 points to the upper Lutetian-lowermost Bartonian (Gradstein et al., 2004).

This line of evidence shows that from late Lutetian to early Priabonian *Sokolowia* is abundantly present from the Tarim Basin to the Transylvanian Basin, occurring essentially across the whole epicontinental sea that covered Eurasia.

4.3.2. Paleoenvironmental analysis

The bivalve assemblages also provide some valuable insight into the paleoecology. *Sokolowia* is characterized by massive, large-sized shells with maximum lengths of ~15 cm. It is a solitary living, epibenthic sediment-recliner and adapted to relatively warm, marine shallow water, above the storm weather wave base (Lan, 1997). It occurs associated with muddy as well as with sandy sea floors. Co-occurring *Kokanostrea* is distinctly smaller and is bounded to hard-grounds, commonly produced by dead and disarticulated *Sokolowia* shells (Lan, 1997). They are colonial, epibenthic, sessile organisms cemented by larger shell to fixed surface (Lan, 1997). For *Flemingostrea* no detailed paleoecological data are available but its co-occurrence with *Kokanostrea* indicates similar preferences.

4.4. Calcareous nannofossils

Calcareous nannofossils have been analyzed from 27 samples from Units 2 to 4 of the Kezi section (Fig. 4). The preparation followed standard techniques (Bown and Young, 1998), quantitative analyses were performed with a light microscope at 1200x magnification and sometimes extended at 400x. In general the assemblages are sparse and the analyses have been extended for at least 400 fields of view. Though we performed an extended analysis, the nannofossils recognized are rare, and the numbers reported in the range chart are the actual specimens encountered (Fig. DR4 and Table DR1).

Four samples are barren, while the remaining 23 could be subdivided in two biofacies, one almost barren of nannofossils, and the other with a rare to very rare content. Abundance and preservation of nannofossils is very much dependent on the lithology, and generally higher in samples from the green mudstones.

4.4.1. Biostratigraphic considerations

In general, our records match those made from sections in the Tarim Basin by Zhong (1992). Particularly their *Discoaster tani nodifer* and *Discoaster saipenensis* Zones compare well to the present record. Hence, it further supports that Units 2 and 3 of the Kezi section represent the Wulagen Formation and not the younger Bashibulake Formation which is characterized by the *Isthmolithus recurvus* Zone according to Zhong (1992).

As nannofossil abundance and preservation are limited, the biostratigraphic attribution is primarily based on both the standard zonations (Gradstein et al., 2004; Okada and Bukry, 1980) and on secondary bioevents in order to constrain the time interval and to make up for the lack of zonal biomarkers (Fig. 4). Biostratigraphic markers included in the standard zonation are *Reticulofenestra umbilicus* (First Occurrence (FO) at the base of CP 14, middle Eocene; Last Occurrence (LO) at the top of CP 16, lower Oligocene) and *Ericsonia formosa* (LO top of CP 16b, lower Oligocene). The occurrence of these markers almost all along the section (Fig. 4), allows the section to be delimited between the base of Zone CP 14 (middle Eocene) and the top of CP 16b (lower Oligocene). The absence of *Isthmolithus recurvus,* which first appears at the base of CP 15b (late Eocene) can further restrict the top of the fossiliferous interval to the earliest Priabonian. Since the sediments have been deposited in a nearshore environment according to lithostratigraphic analyses and various fossil assemblages, the absence of *I. recurvus* is considered reliable since this taxon is regarded tolerant to such conditions (Wei, 1992). The presence of additional markers, i.e. those not indicated in the standard biozonations, can be useful to improve the biostratigraphic resolution. The LO of *Neococcolithes* spp. is reported to occur at the base of CP 15 (upper Eocene; Sheldon, 2002; Varol, 1998). Accordingly, at high southern latitude, Villa et al. (2008) use the LO of *N. dubius* as reliable late Eocene marker for the Southern Ocean, occurring before the FO of *I. recurvus*. The presence of rare and poorly preserved *Blackites inflatus* (LO base of CP 13) are considered reworked as this taxon is never found together with *R. umbilicus*.

Summarizing, based on the interpretation of the calcareous nannofossil distribution, the marine Units 2 and 3 of the Kezi section are assigned to nannofossil Zone CP 14 of Okada and Bukry (1980), which ranges from 41.6 to 37.0 Ma (Fig. 4; Gradstein et al., 2004).

4.4.2. Paleoenvironmental analysis

In general, the low species diversity reflects eutrophic, shallow marine, unstable environments with adverse ecological conditions for coccolithophorids (Aubry, 1992; Bollmann et al., 1993; Brand, 1994; Wade and Bown, 2006). The unusual ‘common’ presence of *Pontosphaera* spp. is reminiscent of a stressed environment with changing or anomalous salinity (Lozar et al., 2009). The presence of holococcoliths (*Neococcolithes, Lanternitus*) bearing structures of rhombohedric crystals are associated with near shore eutrophic conditions. The taxa typically found associated with oligotrophic warm water environments like *Sphenolithus* spp. and *Discoaster* spp. (Chepstow-Lusty et al., 1992) are absent. These interpretations together with the low diversity recorded here, indicate a nearshore, restricted marine setting.

4.5. Palynology

We studied 27 samples from Units 2 and 3 of the Kezi section for palynomorphs (Fig. 4). Out of the 23 samples studied from the Kezi section, 18 yielded palynomorphs, ranging from relatively well to poorly preserved. Productive samples were taken from Units 2 and 3. The preparation followed standardized techniques. Quantitative analysis was performed if preservation state allowed (15 samples), otherwise abundances were roughly estimated (3 samples) using a 400x magnification light microscope. If possible, the analyses have been extended until 200 determinable dinoflagellate cysts were recorded (otherwise, counting was finished after one slide). Taxonomy determinations follow that cited in Fensome and Williams (2004; Fig. DR5 and Table DR2).

4.5.1. Biostratigraphy

Generally, palynological associations are dominated by dinocysts and remains of prasinophyte- and other green algae, while terrestrial palynomorphs (i.e. pollen and spores) are rare. Dinocyst assemblages are diverse with a substantial amount of reworked taxa, primarily of late Cretaceous age (particularly representatives of the *Cyclonephelium* and *Canningia* complex, *Florentinia* spp., *Gonyaulacacysta* spp. and *Hystrichosphaeridium salpingophorum*). Nonetheless, the majority of dinocyst taxa are of Paleogene age. Our records match previous data from the Tarim Basin published by Mao and Norris (1988). In particular their *Turbiosphaera filosa* Zone, with abundant occurrences of taxa recorded typically and globally from the middle and late Eocene like *Areosphaeridium diktyoplokum*, *Charlesdowniea clathrata*, *Diphyes colligerum*, *Glaphyrocysta intricata*, *Rhombodinium draco* and *Wetzeliella* spp, compares well to our record and is regarded typical for the Wulagen Formation. Further age control can be obtained by comparison of the dinocyst distribution from the Kezi section to magnetostratigraphically calibrated records of the Western Mediterranean Tethys in central Italy (Brinkhuis, 1994; Brinkhuis and Biffi, 1993; van Mourik and Brinkhuis, 2005). The presence of *Melitasphaeridium pseudorecurvatum* throughout the Kezi section, allows correlating the top of lithologic Unit 3 of the Kezi section with the top of the Mediterranean *Melitasphaeridium pseudorecurvatum* (Mps) Interval Zone of Brinkhuis and Biffi (1993), which is defined by the Last Occurrence (LO) of this taxon (Fig. 4). This correlation is in agreement with the rare presence of *Cordosphaeridium funiculatum*, which in the Mediterranean Tethys has a First Occurrence (FO) within the Mps Interval Zone. Also the increased abundance of remains of

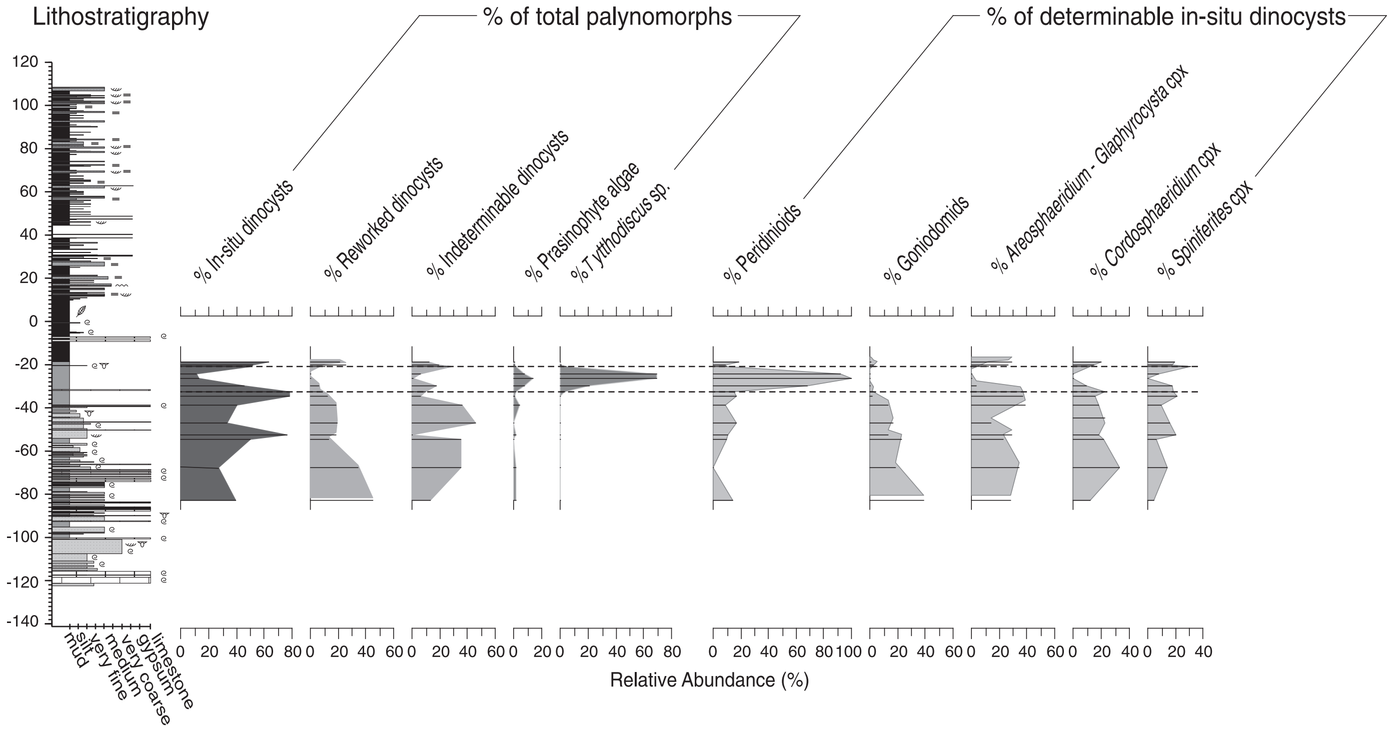

Fig. 5. Relative composition of palynological associations. The left diagrams indicates the relative abundance of non-reworked dinocysts, reworked dinocysts, indeterminable dinocysts and prasinophyte algae which are considered indicative of fresh water influence. The right diagrams indicate the relative abundance of the non-reworked dinocyst taxa: Peridinioid taxa (indicative of eutrophic, fresh water influenced conditions), Goniodomids (lagoonal euryhaline taxa) and other outer neritic taxa. Note the change to a fresh water influenced association between −33 and −21 m level.

prasinophyte algae between the −24 and −30 m level of the Kezi section, correlates with prasinophyte remains that become overwhelmingly dominant in the Western Tethys records throughout the Mps Interval Zone (Fig. 5). The top of this zone has an assigned age of 35.4 Ma (correlative to the top of chron C16n.1n; Fig. 4; Brinkhuis and Biffi, 1993; Gradstein et al., 2004). The base of the Mps Interval Zone is poorly defined. However the presence of *C. funiculatum* leads us to suggest that the investigated interval at Kezi spans the correlative part of this zone in central Italy, of which the exposed base is dated at 37.2 Ma (tied to the base of chron C17n.1n; Fig. 4; Brinkhuis and Biffi, 1993; Gradstein et al., 2004). Hence the age of Units 2 and 3 of the Kezi section is bracketed between 37.2 Ma and 35.4 Ma. Furthermore, the absence of *Schematophora speciosa*, *Stoveracysta ornata* and *Corrudinium?* sp. may indicate that the interval does not include the uppermost part of the Mps Interval Zone, in which these taxa first appear. Therefore we suggest that the most likely age of the uppermost palynologically productive samples of the Kezi section should be somewhat older than 35.4 Ma. The lowest part of the Mps Interval Zone is correlative to the global calcareous nannofossil Zone CP 14 (Fig. 4; Gradstein et al., 2004), which corroborates the interpretations based on calcareous nannofossils.

4.5.2. Paleoenvironmental analysis

With regard to the depositional environment of the Kezi section, palynomorphs indicate a shallow marine environment (<50 m water depth). Goniodomid taxa, as represented here primarily by representatives of the genus *Homotryblium*, are abundant and indicate nearshore, restricted marine and lagoonal conditions (Fig. 5; Brinkhuis, 1994; Pross and Schmiedl, 2002). A proximal depositional environment also manifests itself by the absence of more open oceanic taxa like *Impagidinium* and *Nematosphaeropsis* spp. and relatively high loadings of peridinioid taxa like *Rhombodinium*, *Wetzeliella* and *Deflandrea*. These are likely indicative of increased nutrient availability since in (sub) modern environments, peridinioid taxa primarily represent heterotrophic dinoflagellates and therefore eutrophic conditions (Fig. 5; Powell et al., 1992; Pross and Brinkhuis, 2005; Reichart and Brinkhuis, 2003; Sluijs et al., 2005). The paucity of terrestrial palynomorphs suggests that the continental catchment area was poorly vegetated (in agreement with previous pollen results by Sun and Wang (2005) who inferred that the Tarim Basin was characterized by a relatively arid and warm climate in the Eocene).

Higher order variability is illustrated by the alternation of siliciclastic and carbonate deposits and by the regeneration pulses of ostracod fauna, but is also expressed by quantitative changes in palynological associations (Figs. 4 and 5). Throughout Units 2 and 3 palynological associations reflect a marine dominated lagoonal environment, however, an increased abundance of presumably fresh water tolerant peridinioid dinocysts and prasinophyte algae is recognized below the top of Unit 3, exactly in between the two transgressive pulses indicated by the distribution of ostracod fauna. The nature of this lower intertidal fresh water influenced association is unknown, but it could reflect an increase in fresh water run-off. This near shore incursion close to the top of the marine sequence fits within the recognized trend of shallowing and illustrates how high-frequency sea-level variability is superimposed on this trend.

5. Discussion

The dinocyst-, calcareous nannofossil and bivalve assemblages confirm the lithostratigraphic correlation of the last marine Units 2 to 4 to the Wulagen Formation and hence show that the shallowing upward trend recognized from these lithostratigraphic units represents the (fourth and) last major regression from the Tarim Basin (Figs. 3 and 4; Lan and Wei, 1995; Mao and Norris, 1988; Zhong, 1992). The sequence boundary associated to this regression likely lies between the last marine bed (at 0 m level) and the first continental sandstones (at ~10 m level), close to the boundary between Units 4 and 5 (Fig. 4). The good correlation of this regression between the two

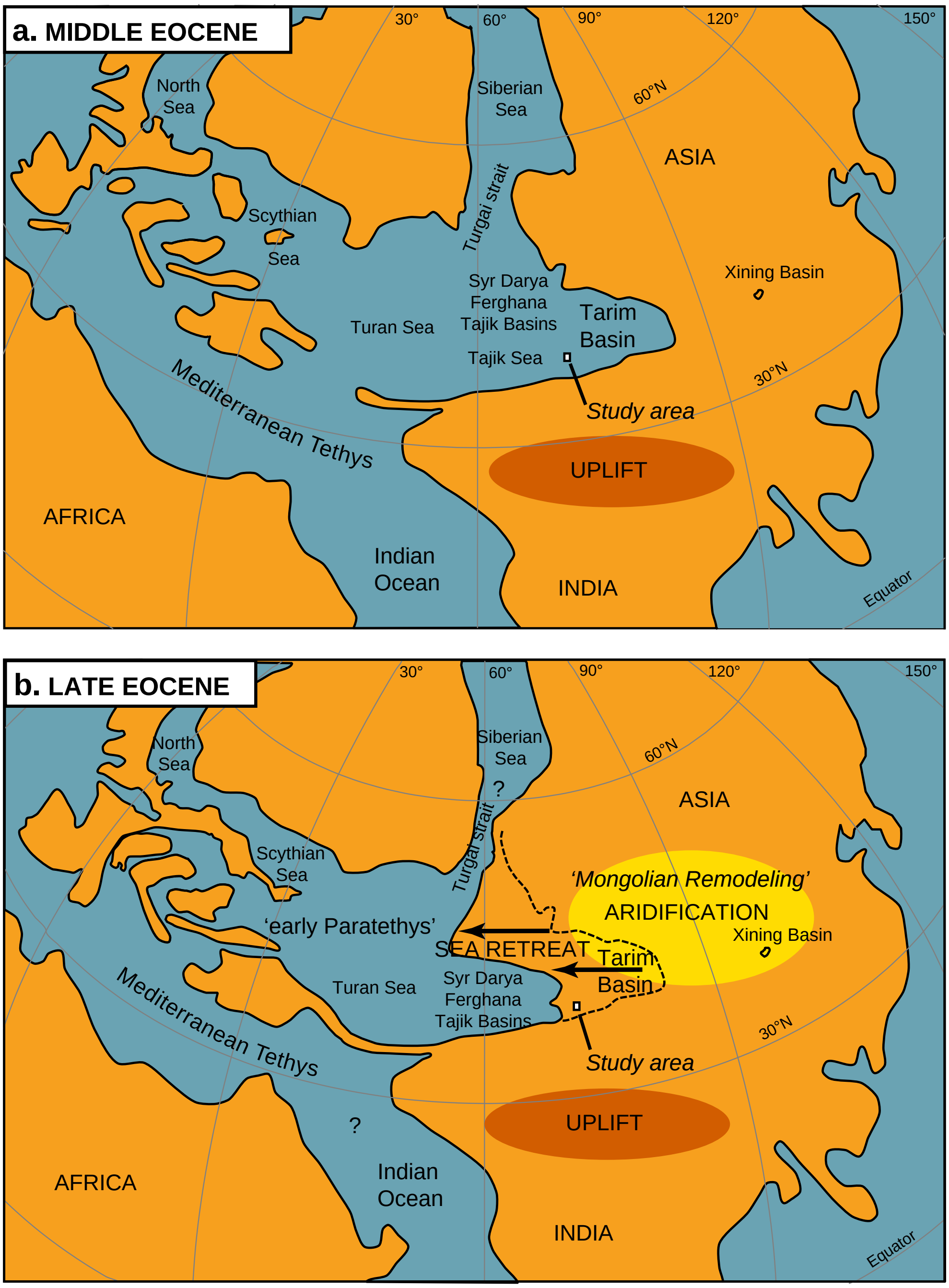

Fig. 6. Paleogeographic maps showing the extent of marine conditions before (a) and after (b) the last major sea retreat from the Tarim Basin, as based upon Popov et al. (2004), Dercourt et al. (1993), Abels et al. (2011) and findings of this study. Plate boundaries were obtained from GPlates 0.9.7.1 for 36 and 34 Ma. The retreat is time equivalent with stepwise aridification reported from the Xining Basin at 36.6 Ma (Abels et al., 2011).

studied sections in terms of lithostratigraphy and bivalve assemblages clearly illustrate that we have documented a regional regression. The best age correlation of the biostratigraphically analyzed interval is based upon assignment to the dinoflagellate Mps Interval Zone (Brinkhuis and Biffi, 1993) and the calcareous nannofossils Zone CP 14, indicating that the uppermost age-diagnostic fossil found at level −17.9 m is older than ~35.4 Ma and that the lowermost age-diagnostic fossil at level −83.2 m is younger than ~41.6 Ma (Fig. 4). These two zonations overlap each other at ~37 Ma according to Gradstein et al. (2004). Since the studied stratigraphic interval comprises a significant part of the recognized shallowing upward trend, chronostratigraphic synthesis of the biostratigraphic results shows that the last major regression out of the Tarim Basin most likely took place during the earliest Priabonian around ~37 Ma. Our stratigraphic framework of Tarim Sea retreat provides significant age control, allowing us to discuss the paleogeography of the sea and both the controlling mechanisms and impacts of this important regression.

5.1. Paleogeography

Our findings now allow us to characterize the marine depositional environment. In general, all biostratigraphic assemblages are indicative of restricted marine, high salinity and lagoonal conditions. We characterize the epicontinental sea of the southwest Tarim Basin as a shallow and proximal marine depositional environment. The recognized paleoenvironmental biomarkers correspond with those of basins to the west, including the neighboring basins of Central Asia and more distant basins of Europe (Fig. 6). Such a resemblance in taxa distribution suggests that these basins were characterized by similar environmental conditions and possibly interconnected.

The late Eocene bivalve assemblages show similarity with macrofossil associations of the Afghan–Tajik Depression, Ferghana Basin and Syr Darya Basin on the opposite side of the Pamir, in perfect agreement with previous studies suggesting that the Tarim Sea is the easternmost extent of the former Turan or Tajik Sea (Fig. 6; Burtman, 2000; Burtman and Molnar, 1993; Dercourt et al., 1993; Lan and Wei, 1995; Popov et al., 2004; Sun, 1991; Tang et al., 1992; Wang and Fu, 1996). Furthermore, the resemblance of the recovered ostracod, bivalve and dinocyst assemblages with assemblages from the northwestern European basins, Transylvanian Basin and the Mediterranean Tethys suggests that surface–ocean connections of the Tarim Basin extended well beyond Central Asia, and that the sea that covered Eurasia during the late Eocene belonged to the Tethyan Realm and had not yet separated as the Paratethys Sea. This assertion is consistent with reported findings of organic-rich and mud-prone sediments in the Black Sea and South Caspian Sea of latest Eocene or early Oligocene age, supposedly indicating the initial isolation and birth of the Paratethys Sea did not occur until that time (Allen and Armstrong, 2008; Báldi, 1984; Dercourt et al., 1993; Popov et al., 2004; Robinson et al., 1996; Rögl, 1999; Rusu, 1985; Schulz et al., 2005; Vincent et al., 2005).

Our biostratigraphy thus confirms that the Tarim Sea was the easternmost extent of a vast epicontinental sea that interconnected the Mediterranean Tethys with various basins of the Eurasian continent, characterized by comparable paleoenvironmental conditions. After supposedly reaching a maximum extent in the early Eocene (Burtman, 2000; Burtman et al., 1996; Lan and Wei, 1995; Tang et al., 1989), the sea retreated from most of the Tarim Basin in the earliest Priabonian. This last major regression was probably part of the longer term westward retreat of the Tarim Sea until it fully disappeared from the Central Asian basins, poorly constrained to late Oligocene time (Fig. 6; Burtman, 2000; Burtman et al., 1996; Coutand et al., 2002).

5.2. Controlling mechanism

The retreat of the Tarim Sea is generally claimed to be controlled by tectonics, as progressive overthrusting of the Pamir mountains and West Kunlun Shan in the Indo-Asia collision system caused sedimentary overfilling and separation of the Tarim Basin from the neighboring Tajik Basin in the west (Fig. 6; Burtman, 2000; Burtman and Molnar, 1993; Coutand et al., 2002; Hao and Zeng, 1984; Lan, 1997; Tang et al., 1992). However, most studies have shown that regional uplift of the Pamir–Kunlun system and other ranges directly surrounding the Tarim Basin paleo-depocentres (Tian Shan and East Kunlun Shan) did not occur until late Oligocene (Burtman, 2000; Robinson et al., 2007; Sobel, 1999; Sobel and Dumitru, 1997; Sobel et al., 2006; Thomas et al., 1994 ; Yang and Liu, 2002), clearly post-dating our inferred early Priabonian sea retreat. The absence of a tectonic barrier, which would prevent the sea on the opposite side of the Pamir from reinvading, is further supported by the reports of short-lived Miocene marine transgressions in both the Afghan–Tajik Depression (Glikman and Ishchenko, 1967) and the Tarim Basin (Graham et al., 2005; Kent-Corson et al., 2009; Ritts et al., 2008). Therefore tectonic closure through the Pamir indentation as a major contributor to the Tarim Sea retreat is considered most unlikely. However, our results do not exclude that the retreat may be (partially) a distal tectonic effect of early Tibetan uplift during the late Eocene (Dai et al., 2006; Dupont-Nivet et al., 2008; Jolivet et al., 2001; Mock et al., 1999; Yang and Liu, 2002; Yin and Harrison, 2000; Yin et al., 2002), characterized by early stage basin infilling and subsidence as suggested by Yin et al. (2002) and Yang and Liu (2002).

Alternatively to a relative -sea-level fall by tectonic uplift, two major Paleogene eustatic sea-level falls were proposed as controlling the last major retreat of the Tarim Basin, but our early Priabonian age clearly shows the retreat pre-dates both the ~70 m Oi-1 eustatic sea-level drop associated to the EOT at ~34 Ma (Katz et al., 2008; Lear et al., 2008; Miller et al., 2005; Pekar et al., 2002) and the mid-Oligocene ~100 m global sea level fall at ~30 Ma (Haq et al., 1987). Other reported sea-level drops, albeit less important, could have contributed to the early Priabonian regression. A short-term global cooling event is reported from early Priabonian oxygen-isotope records of the Southern Ocean (named event C by Villa et al., 2008) and a global sea-level lowstand associated to the Bartonian–Priabonian boundary at ~37.2 Ma (Gradstein et al., 2004) is in good agreement with our inferred timing of the regression at approximately ~37 Ma. Further eustatic control is favored if we focus not only on the fourth regression, but on the complete long-term marine record of the Tarim Basin. It shows that the relative sea-level fluctuations of the five transgression–regression cycles recognized in the Tarim Basin from late Cretaceous to early Oligocene (Fig. 3; Burtman, 2000; Burtman et al., 1996; Lan and Wei, 1995; Tang et al., 1989) correlate reasonably well with the long-term eustatic sea-level curve (Miller et al., 2005; Watts and Steckler, 1979). This implies that long-term sea-level modulated each transgression–regression cycle by determining its extent into the basin (referred to as shifting of the ‘window of opportunity’ by Pratt et al., 1992).

Finally, apart from these allocyclic mechanisms of eustacy and tectonism, shallowing upward cyclicity in shallow epeiric basins like the Paleogene Tarim Basin is often believed to be also controlled partly by autocyclic shoreline progradation (Pratt et al., 1992; Reading, 2006; Schlager, 2005).

Summarizing, we suggest that the last major Tarim Sea retreat of early Priabonian age is a combined expression of its eustatically-driven long-term westward retreat from Central Asia and superimposed short-term autocyclic shoreline progradation, eustatic sea-level lowering and/or tectonically controlled basin-infilling by the early Tibetan uplift.

5.3. Paleoenvironmental impacts

Previous climate modeling studies have shown that the epicontinental sea that extended across Eurasia was the main source of moisture for northwest China and that its retreat would notably increase aridity in that region, possibly enhancing land–sea thermal contrast and strengthening the Asian monsoon (Ramstein et al., 1997; Zhang et al., 2007). Existing records of Asian Paleogene environments do indicate regional aridification north of the Tibetan plateau (Garzione et al., 2005; Graham et al., 2005; Kent-Corson et al., 2009; Sun and Wang, 2005), but poor age constraints on both the aridification records and on the sea retreat precluded testing for a causal relationship. In the Xining Basin along the northeastern Tibetan Plateau (Fig. 6), however, precisely dated pollen bearing playa-lake deposits indicate regional aridification at the 34.0 −33.8 Ma EOT (base of chron C13n; Fig. 4; Dupont-Nivet et al., 2008; Dupont-Nivet et al., 2007; Xiao et al., 2010). Our earliest Priabonian sea retreat from the Tarim Basin is thus clearly not related to the aridification at the EOT, but is conspicuously close to the recently reported major aridification step at 36.6 Ma (top chron C17n.1n) in the Xining Basin by Abels et al. (2011). This preliminary link between the aridification and the sea retreat suggests that the Tarim Sea did function as a major moisture contributor for the Asian interior. However, additional well-dated Asian paleoenvironmental records and improved age control on the Tarim Sea retreat are required to fully establish this link, but also to explore whether later westward retreat of the Turan Sea from Central Asia in the Tarim and Tajik Basins (Burtman, 2000; Burtman et al., 1996; Coutand et al., 2002; Lan and Wei, 1995; Tang et al., 1989) contributed significantly to the Asian aridification at the EOT and to coeval major regional biotic reorganizations such as the Mongolian Remodeling (Böhme, 2007; Kraatz and Geisler, 2010; Meng and McKenna, 1998).

6. Conclusions

During the Paleogene, the Tarim Basin formed the easternmost extend of an epicontinental sea characterized by a shallow, nearshore, restricted marine depositional environment. The Tarim Sea maintained well-established connections with the neighboring basins of Central Asia and was probably part of the Tethyan Realm before the isolation of the Paratethys Sea. The last major regression from the Tarim Basin occurred during the earliest Priabonian (~37 Ma), predating both the tectonic closure of the basin by the Pamir–Kunlun system and the major eustatic sea-level fall of the EOT at ~34 Ma and the mid-Oligocene at ~30 Ma. The Tarim Sea retreat more likely occurred in response to a combination of long-term eustatic sea-level lowering and superimposed short-term eustatic, tectonic and/or autocyclic sedimentary infilling of the basin. It coincides with a significant regional aridification step at ~36.6 Ma in the Xining Basin, suggesting that the Tarim Sea functioned as an important moisture source for the Asian interior.

Supplementary materials related to this article can be found online at doi:10.1016/j.palaeo.2010.11.019.

Acknowledgements

The authors would like to thank Jan van Tongeren for his laboratory assistance and Cor Langereis for his valuable advice and field assistance. This research would not have been possible without funding from the Molengraaff Fund, the Netherlands Organization for Scientific Research (NWO) and Statoil.

References

Abels, H.A., Dupont-Nivet, G., Xiao, G., Bosboom, R., Krijgsman, W., 2011. Step-wise Asian paleoenvironmental changes preceding the Eocene - Oligocene Transition (EOT) in the terrestrial Xining Basin, China. Palaeogeography, Palaeoclimatology, Palaeoecology 299, 399–412.

Aigner, T., Brandenburg, A., van Vliet, A., Lawrence, D., Westrich, J., 1990. Stratigraphic modelling of epicontinental basins: two applications. Sedimentary Geology 69, 167–190.

Allen, M.B., Armstrong, H.A., 2008. Arabia-Eurasia collision and the forcing of mid-Cenozoic global cooling. Palaeogeography, Palaeoclimatology, Palaeoecology 265 (1–2), 52–58.

Aubry, M.P., 1992. Late Paleogene calcareous nannoplankton evolution: a tale of climatic deterioration. In: Prothero, D.R., Berggren, W.A. (Eds.), Eocene–Oligocene Climatic and Biotic Evolution. Princeton University Press, pp. 272–309.

Báldi, T., 1984. The terminal Eocene and Early Oligocene events in Hungary and the separation of an anoxic, cold Paratethys. Eclogae Geologocae Helvetiae 77, 1–27.

Berizzi Quarto di Palo, A., 1970. Paleogene pelecypods from Kataghan and Badakhshan (North-East Afganistan). In: Desio, A. (Ed.), Fossils of North-East Afganistan: Italian Expeditions to the Karakorum (K2), and Hindu Kush, IV/2:. Brill, Leiden, pp. 161–240.

Über cretaceische und eocäne Versteinerungen aus Fergana. In: Böhm, J. (Ed.), Durch Asien, Band 3. Reimer, Berlin. 95-111 pp.

Böhme, M., 2007. Oligocene-Miocene Vertebrates from the Valley of Lakes (Central Mongolia): morphology, phylogenetic and stratigraphic implications. - 3. Herpetofauna (Anura, Squamata) and palaeoclimatic implications: preliminary results. Annalen des Naturhistorischen Museums Wien 108A, 43–52.

Bollmann, J., Hilbrecht, H., Thierstein, H.R., 1993. Evenness and species-richness in modern coccolith and foraminifera assemblages. International Nannoplankton Association Newsletter 15/ 2 (55).

Bombita, G., Rusu, A., 1981. New data on the Eocene/Oligocene boundary in the Romanian Carpathians. Palaeogeography, Palaeoclimatology, Palaeoecology 36 (3–4), 213–222.

Boos, W.R., Kuang, Z., 2010. Dominant control of the South Asian monsoon by orographic insulation versus plateau heating. Nature 463, 218–223.

Bown, P.R., Young, J.R., 1998. Introduction. In: Bown, P.R. (Ed.), Calcareous Nannofossil Biostratigraphy: British Micropalaeontology Society Series. Chapman and Hall, London, pp. 1–15.

Brand, L.E., 1994. Physiological ecology of marine coccolithophores. In: Winter, A., Siesser, W.G. (Eds.), Coccolithophores. Cambridge University Press, Cambridge, pp. 39–49.

Brinkhuis, H., 1994. Late Eocene to Early Oligocene dinoflagellate cysts from the Priabonian type-area (Northeast Italy): biostratigraphy and paleoenvironmental interpretation. Palaeogeography, Palaeoclimatology, Palaeoecology 107 (1–2), 121–163.

Brinkhuis, H., Biffi, U., 1993. Dinoflagellate cyst stratigraphy of the Eocene/Oligocene transition in central Italy. Marine Micropaleontology 22 (1–2), 131–183.

Carbonate-siliciclastic mixtures. In: Budd, D.A., Harris, P.M. (Eds.), SEPM Reprint Series Number 14. SEPM, Tulsa, Oklahoma. 272 pp.

Bugrova, E.M., 2009. Paleogen Turkmenistana (Obnovlenaja shema zonaljnogo raschlenenija i korrelacii). Neftegasovaa geologia. Teoria i praktika 4, 1–32.

Bureau of Geology and Mineral Resources of Xinjiang Uygur Autonomous Region, 1993. Regional Geology of Xinjiang Uygur Autonomous Region. Geological Publishing House, Beijing. 1841 pp.

Burtman, V.S., 2000. Cenozoic crustal shortening between the Pamir and Tien Shan and a reconstruction of the Pamir–Tien Shan transition zone for the Cretaceous and Palaeogene. Tectonophysics.

Burtman, V.S., Molnar, P., 1993. Geological and geophysical evidence for deep subduction of continental crust beneath the Pamir. Geological Society of America Special Paper 281, 76p.

Burtman, V.S., Skobelev, S.F., Molnar, P., 1996. Late Cenozoic slip on the Talas-Ferghana fault, the Tien Shan, central Asia. Geological Society of America Bulletin 108 (8), 1004.

Chepstow-Lusty, A., Backman, J., Shackleton, N.J., 1992. Comparison of Upper Pliocene Discoaster abundance variations from the Atlantic, Pacific and Indian Oceans: the significance of productivity pressure at low latitudes. Memorie di Scienze Geologiche 44, 357–373.

Cita, M.B., Premoli Silva, I., 1975. Micropaleontological notes on some Cretaceous-Eocene sections in North-Eastern Afghanistan. In: Desio, A. (Ed.), Geology of Central Badakhshan: Italian Expeditions to the Karakorum (K2), and Hindu Kush. Brill, Leiden, pp. 457–494.

Coutand, I., et al., 2002. Late Cenozoic tectonic development of the intramontane Alai Valley, (Pamir-Tien Shan region, central Asia): an example of intracontinental deformation due to the Indo-Eurasia collision. Tectonics 21 (6), 1–19.

Cowgill, E., 2010. Cenozoic right-slip faulting along the eastern margin of the Pamir salient, northwestern China. Geological Society of America Bulletin 122, 145–161.

Coxall, H.K., Wilson, P.A., Palike, H., Lear, C.H., Backman, J., 2005. Rapid stepwise onset of Antarctic glaciation and deeper calcite compensation in the Pacific Ocean. Nature 433 (7021), 53–57.

Dai, S., et al., 2006. Magnetostratigraphy of Cenozoic sediments from the Xining Basin: tectonic implications for the northeastern Tibetan Plateau. Journal of Geophysical Research 111, B11102. doi:10.1029/2005JB004187.

Atlas Tethys paleoenvironmental maps. In: Dercourt, J., Ricou, L.E., Vrielynck, B. (Eds.), Commision for the Geological Map of the World, Paris. 269 pp.

Desio, A., Martina, E., 1975. Some stratigraphical sequences of Katagan and surrounding regions. In: Desio, A. (Ed.), Geology of Central Badakhshan: Italian Expeditions to the Karakorum (K2), and Hindu Kush. Brill, Leiden.

Ducasse, O., Guernet, C., Ambareau, Y., 1985. Paléogène. In: Oertli, H.J. (Ed.), Atlas des Ostracodes de France: Bull. Centres Rech. Explor.-Prod. Elf-Aquitaine, pp. 257–311.

Dupont-Nivet, G., Guo, Z., Butler, R.F., Jia, C., 2002. Discordant paleomagnetic direction in Miocene rocks from the central Tarim Basin: evidence for local deformation and inclination shallowing. Earth and Planetary Science Letters 199, 473–482.

Dupont-Nivet, G., Hoorn, C., Konert, M., 2008. Tibetan uplift prior to the Eocene-Oligocene climate transition: evidence from pollen analysis of the Xining Basin. Geology 36 (12), 987–990. doi:10.1130/GS25063A.1.

Dupont-Nivet, G., et al., 2007. Tibetan plateau aridification linked to global cooling at the Eocene-Oligocene transition. Nature 445 (7128), 635–638.

Escutia, C., Brinkhuis, H., Klaus, A., 2010. Cenozoic east Antarctic ice sheet evolution from Wilkes Land margin sediments. Integrated Ocean Drilling Program Expedition, p. 318.

Fensome, R.A., Williams, G.L., 2004. The Lentin and Williams index of fossil dinoflagellates. American Association of Stratigraphic Palynologists Foundation Contr. Series.

Garzione, C., Ikari, M.J., Basu, A.R., 2005. Source of Oligocene to Pliocene sedimentary rocks in the Linxia basin in northeastern Tibet from Nd isotopes: implications for tectonic forcing of climate. Geological Society of America Bulletin 117 (9), 1156–1166. doi:10.1130/B25743.1.

Glikman, L.S., Ishchenko, V.V., 1967. Marine Miocene sediments in Central Asia.. Doklady Akademii NAUK SSSR. Geology 177, 78–81.

Gorizdro, S.F., 1913. Material for the Tertiary Turkestan fauna study: Trudy Imperatorskago Sankt-Peterburgskago Obshchestva Estestvoispytateley. Otdelenie geologii i mineralogii 37 (5), 1–57.

Gradstein, F.M., Ogg, J.G., Smith, A.G., 2004. The Geomagnetic Polarity Time Scale. A geologic time scale 2004. Cambridge University Press, Cambridge. 589 pp.

Graham, S.A., et al., 2005. Stable isotope records of Cenozoic climate and topography, Tibetan plateau and Tarim basin. American Journal of Science 305 (2), 101–118.

Guo, X., 1991. An approach to the depositional environment of the Cretaceous Kizilsu Group: The lowermost marine horizon of the Cretaceous in the western Tarim Basin. Acta Geological Sinica 2, 188–198.

Hao, Y.C., Zeng, X.L., 1984. On the evolution of the west Tarim gulf from Mesozoic to Cenozoic in terms of characteristics of foraminiferal fauna. Acta Micropalaeontologica Sinica 1 (1), 1–13.

Haq, B.U., Hardenbol, J., Vail, P.R., 1987. Chronology of fluctuating sea levels since the Triassic. Science 235 (4793), 1156.

Hendrix, M.S., et al., 1992. Sedimentary record and climatic implications of recurrent deformation in the Tian Shan: evidence from Mesozoic strata of the north Tarim, south Junggar, and Turpan basins, northwest China. Geological Society of America Bulletin 53–79.

Hu, B., 1992. Petroleum geology and prospects of the Tarim (Talimu) Basin, China. In: Halbouty, M.T. (Ed.), Giant Oil and Gas Fields of the Decade 1978-1988. American Association of Petroleum Geologists, Tulsa, pp. 493–510.

Jia, C., Wei, G., Wang, L., Jia, D., Guo, Z. (Eds.), 1997. Tectonic Characteristics and Petroleum, Tarim Basin, China. Petroleum Industry Press, Beijing. 295 pp.

Jia, C., Zhang, S., Wu, S., 2004. Stratigraphy of the Tarim Basin and Adjacent Areas. Science Press, Beijing. 540 pp.

Jin, X., Wang, J., Chen, B., Ren, L., 2003. Cenozoic depositional sequences in the piedmont of the west Kunlun and their paleogeographic and tectonic implications. Journal of Asian Earth Sciences 21 (7), 755–765.

Jolivet, M., et al., 2001. Mesozoic and Cenozoic tectonics of the northern edge of the Tibetan Plateau: fission-track constraints. Tectonophysics 343 (1–2), 111–134.

Katz, M.E., et al., 2008. Stepwise transition from the Eocene greenhouse to the Oligocene icehouse. Nature Geoscience 1 (5), 329–334.

Keen, M.C., 1978. The Tertiary- Paleogene. In: Bate, R.H., Robinson, E. (Eds.), A Stratigraphical Index of British Ostracoda. Seel House Press, Liverpool, pp. 385–449.

Keij, A.J., 1957. Eocene and Oligocene Ostracoda of Belgium. Mem. Inst. Roy. Sci. Nat, Belgique, Bruxelles. 136 pp.

Kent-Corson, M.L., et al., 2009. Stable isotopic constraints on the tectonic, topographic, and climatic evolution of the northern margin of the Tibetan Plateau. Earth and Planetary Science Letters 282 (1–4), 158–166.

Kraatz, B.P., Geisler, J.H., 2010. Eocene-Oligocene transition in Central Asia and its effects on mammalian evolution. Geology 38 (2), 111–114.

Kutzbach, J.E., Geutter, P.J., Ruddiman, W.F., Prell, W.L., 1989. Sensitivity of climate to Late Cenozoic uplift in southern Asia and the Amercian west: numerical experiments. Journal of Geophysical Research 94, 18,393–18,407.

Lan, X., 1997. Paleogene bivalve communities in the western Tarim Basin and their paleoenvironmental implications. Paleoworld 7, 137–157.

Lan, X., Wei, J. (Eds.), 1995. Late Cretaceous-Early Tertiary Marine Bivalve Fauna from the Western Tarim Basin. Chinese Science Publishing House, Beijing. 212 pp.

Lear, C.H., Bailey, T.R., Pearson, P.N., Coxall, H.K., Rosenthal, Y., 2008. Cooling and ice growth across the Eocene-Oligocene transition. Geology 251–254.

Lozar, F., et al., 2009. Calcareous nannofossils herald the Messinian salinity crisis: the Pollenzo section (Alba, Cuneo; NW Italy). Geobios 43 (1), 21–32.

Mao, S., Norris, G., 1988. Late Cretaceous-early Tertiary dinoflagellates and acritarchs from the Kashi area, Tarim Basin, Xinjiang Province, China. Life Science Contributions, 150. Royal Ontario Museum. 93 pp.

Meng, J., McKenna, M.C., 1998. Faunal turnovers of Palaeogene mammals from the Mongolian Plateau. Nature 394, 364–367.

Meszaros, N., 1957. Fauna de Moluste a depozitelor Paleogene din Nord-Vestul Transilvaniei. Monografii de Geologie se Paleontologie 1 Bucuresti, 1-174 pp.

Miller, K.G., et al., 2005. The Phanerozoic record of global sea-level change. Science 310 (5752), 1293–1298.

Mock, C., Arnaud, N., Cantagrel, J.-M., 1999. An early unroofing in northeastern Tibet? Constraints from 40Ar/39Ar thermochronology on granitoids from the eastern Kunlun range (Qinghai, NW China). Earth and Planetary Science Letters 171, 107–122.

Murray, J.W., 1991. Ecology and Palaeoecology of Benthic Foraminifera. Longman, London. 397 pp.

Oertli, H.J., 1956. Ostracoden aus der oligozänen und miocänen Molasse der Schweiz. Schweizerische Paläontologische Abhandlungen 74, 1–119.

Okada, H., Bukry, D., 1980. Supplementary modification and introduction of code numbers to the low latitude coccolith biostratigraphic zonation (Bukry 1973, 1975). Marine Micropaleontology 5, 321–325.

Olteanu, R., 2006. Monografia ostracodelor tertiare din arealul carpatic. Editura Academei Romane, Bucuresti. 239 pp.

Pagani, M., Zachos, J.C., Freeman, K.H., Tipple, B., Bohaty, S., 2005. Marked decline in atmospheric carbon dioxide concentrations during the Paleogene. Science 309 (5734), 600–603.

Pavay, E., 1871. Kolozsvar környekenek földtani viszonyai:. A Magyar Kiralyi Földtani Intezet Evkönyve 1, 327–462.

Pearson, P.N., Foster, G.L., Wade, B.S., 2009. Atmospheric carbon dioxide through the Eocene–Oligocene climate transition. Nature 461, 1110–1113.

Pekar, S.F., Christie-Blick, N., Kominz, M.A., Miller, K.G., 2002. Calibration between eustatic estimates from backstripping and oxygen isotopic records for the Oligocene. Geology 30 (10), 903.

Pietrzeniuk, E., 1969. Taxonomische und biostratigraphishe Untersuchungen an Ostracoden des Eozän 5 im Norden der Deutschen Demokratischen Republik, Bd. IV (1). Pal. Abh. Paläzoologie, Berlin. . 139 pp.

Popov, S., et al., 2004. Lithological-Paleogeographic maps of Paratethys 10 Maps Late Eocene to Pliocene. Courier Forschungsinstitut Senckenberg 250, 1–42.

Powell, A.J., Lewis, J., Dodge, J.D., 1992. The palynological expressions of post-Palaeogene upwelling: a review. Upwelling Systems: Evolution Since the Early Miocene, pp. 215–226.

Pratt, B.R., James, N.P., Cowan, C.A., 1992. Peritidal carbonates. In: Walker, R.G., James, N.P. (Eds.), Facies Models: Response to Sea Level Change. Geological Association of Canada, St John's, Newfoundland, p. 409.

Prell, W.L., Kutzback, J.E., 1992. Sensitivity of the Indian monsoon to forcing parameters and implications for its evolution. Nature 360, 647–652.

Premoli Silva, I., 1970. Cretaceous-Eocene microfaunas from Western Badakhshan and Kataghan (North-East Afganistan). In: Desio, A. (Ed.), Fossils of North-East Afganistan: Italian Expeditions to the Karakorum (K2), and Hindu Kush. Brill, Leiden, pp. 119–160.

Pross, J., Brinkhuis, H., 2005. Organic-walled dinoflagellate cysts as paleoenvironmental indicators in the Paleogene; a synopsis of concepts. Paläontologische Zeitschrift 79 (1), 53–59.

Pross, J., Schmiedl, G., 2002. Early Oligocene dinoflagellate cysts from the Upper Rhine Graben (SW Germany): paleoenvironmental and paleoclimatic implications. Marine Micropaleontology 45 (1), 1–24.

Ramstein, G., Fluteau, F., Besse, J., Joussaume, S., 1997. Effect of orogeny, plate motion and land–sea distribution on Eurasian climate change over the past 30 million years. Nature 386, 788–795.

Reading, H.G. (Ed.), 2006. Sedimentary Environments: Processes, Facies and Stratigraphy. Blackwell Publishing Inc., Oxford. 688 pp.

Reichart, G.J., Brinkhuis, H., 2003. Late Quaternary Protoperidinium cysts as indicators of paleoproductivity in the northern Arabian Sea. Marine Micropaleontology 49 (4), 303–315.

Ritts, B.D., et al., 2008. From sea level to high elevation in 15 million years:uplift history of the northern Tibetan Plateau margin in the Altun Shan. American Journal of Science 308 (5), 657–678.

Robinson, A.C., et al., 2007. Cenozoic evolution of the eastern Pamir: implications for strain-accommodation mechanisms at the western end of the Himalayan-Tibetan orogen. Geological Society of America Bulletin 882–896.

Robinson, A.G., Rudat, J.H., Banks, C.J., Wiles, R.L.F., 1996. Petroleum geology of the Black Sea. Marine and Petroleum Geology 13 (2), 195–223.

Robinson, D.M., Dupont, N.G., Gehrels, G.E., Zhang, Y., 2003. The Tula Uplift, northwestern China; evidence for regional tectonism of the northern Tibetan Plateau during late Mesozoic-early Cenozoic time. Geological Society of America Bulletin 115 (1), 35–47.

Rögl, F., 1999. Short note: Mediterranean and Paratethys. Facts and hypotheses of an Oligocene to Miocene paleogeography (short overview). Geologica Carpathica 50 (4), 339–349.

Romanovskiy, G., 1880. Materialien zur Geologie von Turkestan. 1. Lieferung. Geologische und Paläontologische Uebersicht des Nordwestlichen Thian-Schan und des Südöstlichen Theiles der Niederung von Turan. Acad. Wissenschaften, St.-Petersburg. 143 pp.

Rossi Ronchetti, C., 1975. Megafossils of some localities of North-Eastern Afghanistan. In: Desio, A. (Ed.), Geology of Central Badakhshan. - Italian Expeditions to the Karakorum (K2), and Hindu Kush. Brill, Leiden, pp. 509–520.

Ruddiman, W.F., Kutzbach, 1989. Forcing of Late Cenozoic northern hemisphere climate by plateau uplift in southern Asia and the American west. Journal of Geophysical Research 94 (18), 409–18427.

Rusu, A., 1985. Oligocene events in Transylvania (Roumania) and the first separation of Paratethys. Dari de Seama ale Sedintelor Institutul de Geologie si Geofizica 72–73, 207–223.

Rusu, A., Brotea, D., Melinte, M.C., 2004. Biostratigraphy of the Bartonian deposits from Gilău area (NW Transylvania, Romania). Acta Palaeontologica Romaniae 4, 441–454.

Scheremeta, V., 1969. Ostracodi Paleogena Ucraini. Iz. Lvovskogo Univ, Lvov. 250 pp.

Schlager, W., 2005. Carbonate sedimentology and sequence stratigraphy. Concepts in Sedimentology and Paleontology, 8. SEPM. 200 pp.

Schulz, H.-M., Bechtel, A., Sachsenhofer, R.F., 2005. The birth of the Paratethys during the Early Oligocene: from Tethys to an ancient Black Sea analogue? Global and Planetary Change 49 (3–4), 163–176.

Sheldon, E., 2002. Palaeogene nannofossil biostratigraphy of the Kangâmiut-1 and Nukik-2 wells, offshore West Greenland. Marine and Petroleum Geology 20, 1031–1041.

Sluijs, A., Pross, J., Brinkhuis, H., 2005. From greenhouse to icehouse; organic-walled dinoflagellate cysts as paleoenvironmental indicators in the Paleogene. Earth Science Reviews 68 (3–4), 281–315.

Sobel, E.R., 1999. Basin analysis of the Jurassic-Lower Cretaceous southwest Tarim basin, northwest China. Geological Society of America Bulletin 709–724.

Sobel, E.R., Chen, J., Heermance, R.V., 2006. Late Oligocene-Early Miocene initiation of shortening in the Southwestern Chinese Tian Shan: implications for Neogene shortening rate variations. Earth and Planetary Science Letters 247 (1–2), 70–81.

Sobel, E.R., Dumitru, T.A., 1997. Thrusting and exhumation around the margins of the western Tarim basin during the India-Asia collision. Journal of Geophysical Research 102 (B3), 5043–5063.

Stenzel, H.B., 1971. Oysters. In: Moore, R.C. (Ed.), Treatise on Invertebrate Paleontology. Geological Society of America and University of Kansas Press, Boulder (Colorado), pp. 953–1224.

Sun, D.L., 1991. Late Cretaceous-Early Tertiary Gastropods, Echinoids and Brachiopods from the Western Tarim Basin, South Xinjiang, China. Science Press, Beijing. 150 pp.

Sun, X., Wang, P., 2005. How old is the Asian monsoon system? Palaeobotanical records from China. Palaeogeography, Palaeoclimatology, Palaeoecology 222, 181–222.

Szczechura, J., 1977. Ostracods from the Upper Eocene of East Poland. Acta Palaeontologica Polonica 22 (1), 55–92.

Tang, T., Xue, Y., Yu, C., 1992. Characteristics and sedimentary environments of the Late Cretaceous to early Tertiary marine strata in the western Tarim, China. Science Press, Beijing. 138 pp.

Tang, T., et al., 1989. Marine Late Cretaceous and Early Tertiary Stratigraphy and Petroleum Geology in Western Tarim Basin, China. Science Press, Beijing. 141 pp.

Thomas, J.-C., et al., 1994. Paleomagnetic evidence for Cenozoic block rotations in the Tadjick depression (Central Asia). Journal of Geophysical Research 99, 15141–15160.

Tian, Z., Chai, G., Kang, Y., 1989. Tectonic evolution of the Tarim basin. In: Zhu, X. (Ed.), Chinese Sedimentary Basins. : Sedimentary Basins of the World. Elsevier, Amsterdam, pp. 33–42.

van Morkhoven, F.P.C.M., 1963. Post-Paleozoic ostracoda. Their Morphology, Taxonomy and Economic Use, I and II. Elsevier Publ. Co, Amsterdam-London-New York. 204 and 478 pp.

van Mourik, C.A., Brinkhuis, H., 2005. The Massignano Eocene-Oligocene golden spike section revisited. Stratigraphy 2, 13–29.
Varol, 1998. Palaeogene. In: Brown, P.R. (Ed.), Calcareous Nannofossil Biostratigraph y British Micropal. Chapman & Hall/Kluwer Academic, New York, pp. 200–224.
Villa, G., Fioroni, F., Pea, L., Bohaty, S., Persico, D., 2008. Middle Eocene–late Oligocene climate variability: calcareous nannofossil response at Kerguelen Plateau, Site 748. Marine Micropaleontology 69, 173–192.
Vincent, S.J., et al., 2005. Insights from the Talysh of Azerbaijan into the Paleogene evolution of the South Caspian region. GSA Bulletin 117, 1513–1533.
Vyalov, O.S., 1935. Shema delenija tretchnih otlozheni Fergani. C.R. Acad. Sci. URSS, Leningrad, pp. 278–281.
Vyalov, O.S., 1937. Sur la Clasification des Ostreides et leur Valeur stratigraphique. Intern. Congr. Zool. 1627–1638 Lisbonne.
Wade, B.S., Bown, P.R., 2006. Calcareous nannofossils in extreme environment: the Messinian Salinity Crisis, Polemi Basin, Cyprus. Palaeogeography, Palaeoclimatology, Palaeoecology 233, 271–286.
Wang, Y., Fu, D., 1996. The sedimentary-tectonic evolution of the southwest Tarim basin from Cretaceous to Paleogene. Acta Geologica Sinica 17, 32–40.
Watts, A.B., Steckler, M.S., 1979. Subsidence and eustasy at the continental margin of eastern North America. Deep drilling results in Atlantic Ocean: Continental margins and paleoenvironment. Maurice Ewing Series, 3. American Geological Union, Washington, D. C., pp. 218–234.
Updated nannofossil stratigraphy of the Ciros-1 Core from Mcmurdo Sound (Ross Sea). In: Wei, W. (Ed.), Proceedings of the Ocean Drilling Program: Scientific Results 120 1105-1117 pp.
Xiao, G., Abels, H.A., Yao, Z., Dupont-Nivet, G., Hilgen, F.J., 2010. Asian aridification linked to the first step of the Eocene-Oligocene climate Transition (EOT) in obliquity-dominated terrestrial records (Xining Basin, China). Climate of the Past.
Yang, H., Jiang, X., Lin, S., 1995. Late Cretaceous- Early Tertiary Ostracod Fauna from Western Tarim Basin, South Xinjiang, China, Beijing. 173 pp.
Yang, Y., Liu, M., 2002. Cenozoic deformation of the Tarim plate and the implications for mountain building in the Tibetan plateau and the Tian Shan. Tectonics 21 (6), 1059.
Yeşilyurt, N., Tunoğlu, C., Ertekin, İ., 2009. Ostracoda assemblage and environmental interpretation of the Bartonian-Priabonian Seydiler Formation (Kastamonu-Northern Turkey). Geological Bulletin of Turkey 52 (1), 20–85.
Yin, A., Harrison, M.T., 2000. Geologic evolution of the Himalayan-Tibetan orogen. Annual Review of Earth and Planetary Sciences 28, 211–280.
Yin, A., et al., 2002. Tectonic history of the Altyn Tagh fault system in northern Tibet inferred from Cenozoic sedimentation. Geological Society of America Bulletin 114 (10), 1257–1295.
Zhang, Z., Wang, H., Guo, Z., Jiang, D., 2007. What triggers the transition of palaeoenvironmental patterns in China, the Tibetan Plateau uplift or the Paratethys Sea retreat? Palaeogeography, Palaeoclimatology, Palaeoecology 245 (3–4), 317–331.
Zheng, H., Huang, X., Butcher, K., 2006. Lithostratigraphy, petrography and facies analysis of the Late Cenozoic sediments in the foreland basin of the West Kunlun. Palaeogeography, Palaeoclimatology, Palaeoecology 241, 61–78.
Zhong, S., 1992. Calcareous Nannofossils from the Upper Cretaceous and Lower Tertiary in the Western Tarim Basin, South Xinjiang, China. Chinese Science Publishing House, Beijing. 121 pp.